A&A 404, 775–781 (2003)
DOI: 10.1051/0004-6361:20030499

Astronomy & Astrophysics

Multi-order TODCOR: Application to observations taken with the CORALIE echelle spectrograph

I. The system HD 41004⋆,⋆⋆

S. Zucker[1,2], T. Mazeh[1], N. C. Santos[3], S. Udry[3], and M. Mayor[3]

[1] School of Physics and Astronomy, Raymond and Beverly Sackler Faculty of Exact Sciences, Tel Aviv University, Tel Aviv, Israel
[2] *Present address:* Dept. of Geophysics and Planetary Sciences, Raymond and Beverly Sackler Faculty of Exact Sciences, Tel Aviv University, Tel Aviv, Israel
[3] Observatoire de Genève, 51 ch. des Maillettes, 1290 Sauverny, Switzerland

Received 2 January 2003 / Accepted 25 February 2003

Abstract. This paper presents an application of the TwO-Dimensional CORrelation (TODCOR) algorithm to multi-order spectra. The combination of many orders enables the detection and measurement of the radial velocities of very faint companions. The technique is first applied here to the case of HD 41004, where the secondary is 3.68 mag fainter than the primary in the V band. When applied to CORALIE spectra of this system, the technique measures the secondary velocities with a precision of 0.6 km s^{-1} and facilitates an orbital solution of the HD 41004 B subsystem. The orbit of HD 41004 B is nearly circular, with a companion of a 19 M_J minimum mass. The precision achieved for the primary is 10 m s^{-1}, allowing the measurement of a long-term trend in the velocities of HD 41004 A.

Key words. methods: data analysis – techniques: radial velocities – stars: binaries: spectroscopic – stars: individual: HD 41004 – stars: low-mass, brown dwarfs

1. Introduction

TODCOR (TwO-Dimensional CORrelation) is a two-dimensional correlation technique to derive the radial velocities of both components of double-lined binary spectra (Zucker & Mazeh 1994). It was introduced as a generalization of the (one-dimensional) cross-correlation technique (Simkin 1974; Tonry & Davis 1979) to deal with the difficulties encountered in double-lined spectra, when the lines of the two components cannot be easily resolved. Assuming the observed spectrum is a combination of two known spectra shifted by the radial velocities of the two components, TODCOR calculates the correlation of the observed spectrum against a combination of two templates with different shifts. The result is a two-dimensional correlation function, whose peak simultaneously identifies the radial velocities of both the primary and the secondary.

One of the advantages of TODCOR is its ability to use different templates for the primary and the secondary. When the primary and the secondary are of different spectral types, the simultaneous use of two different templates utilizes all the spectral information contained in the observed spectrum of the combined system. This feature of TODCOR is most important when deriving the radial velocities of faint secondaries (Mazeh & Zucker 1994). However, the ability to detect faint secondaries using TODCOR is still limited, depending mainly on the signal-to-noise ratio and the number of spectral lines. Therefore, Mazeh et al. (2002) and Prato et al. (2002), who searched for faint companions, had to apply TODCOR on IR spectra, where the flux ratio is favorable for detecting cooler stars.

The modern spectrographs offer another path to enhance the ability to detect faint companions. Due to the progress in detector technology, many of the modern spectrographs produce multi-order spectra. In order to enhance our ability to detect a faint companion, while maximizing the precision of the measured velocities, we need to combine the spectral information in all the relevant orders. Originally, TODCOR was devised to analyse only single-order spectra, and further

Send offprint requests to: S. Zucker,
e-mail: shay@wise.tau.ac.il

⋆ Based on observations collected at the La Silla Observatory, ESO (Chile), with the CORALIE spectrograph at the 1.2-m Euler Swiss telescope

⋆⋆ Table 4 is only available in electronic form at the CDS via anonymous ftp to cdsarc.u-strasbg.fr (130.79.128.5) or via http://cdsweb.u-strasbg.fr/cgi-bin/qcat?J/A+A/404/775

generalization is therefore needed in order to use the information in multiple orders.

When applying TODCOR to each order separately, the weak signal of the secondary may produce a certain local peak of the correlation function at the correct secondary velocity. However, this peak can be easily topped by spurious random peaks. This rules out, for example, calculation of the radial velocity independently for each order and then averaging the velocities, since many of the secondary velocities would have resulted from wrong peaks. Concatenation of the spectral orders to one single spectrum would require special treatment to the gaps and overlaps between adjacent orders. Co-adding overlapping regions and bridging the gaps both require interpolation, which would introduce artificial noise into the analysed spectrum.

The approach we suggest here is to calculate the correlation function for each order separately, and then combine the correlation functions of all the orders. The combination emphasizes the relevant correlation peak, and averages out the spurious random peaks. A simple average of the correlation functions may not be efficient enough, since the combination scheme has to consider the different spectral information in the different orders, and weigh them accordingly. Zucker (2003) introduces such a scheme, based on a few plausible statistical assumptions.

Using this scheme, multi-order TODCOR is applied in this work to the CORALIE spectra of HD 41004. As Santos et al. (2002) have shown, these spectra are composed of the spectra of the two visual components of the system, that are separated by 0.5″. Santos et al. found that the radial velocities measured by CORALIE for these spectra showed a minute periodical variability. They suggested that this apparent variation was actually related to a much larger variation in the velocity of the faint B component. The presence of the spectrum of HD 41004 B caused a variable asymmetry in the line shape of the composite spectra, which was reflected in a minute variability of the measured radial velocity.

TODCOR, when applied to the multi-order CORALIE spectra of HD 41004, derived the radial velocities of *both* components without any assumptions regarding the orbit. The derived velocities confirm the conjecture of Santos et al.: the B component indeed moves periodically with a 1.3-day period, and the A component shows a long-term trend. We present here an orbital solution for the B component and derive the slope of the long-term trend of the A component, based on the precise velocities derived by TODCOR.

The next section briefly reviews the previous results concerning HD 41004. The analysis and its results are presented in Sects. 3 and 4. Section 5 discusses the results and their implications. Section 6 concludes the paper with a few remarks.

2. Characteristics of HD 41004

HD 41004 is a visual double system, consisting of a K1V–M2V pair. According to the Hipparcos catalogue, the pair is a common-proper-motion pair, with a V-magnitude difference of 3.68 and a separation of $0.541'' \pm 0.033''$. The basic stellar parameters of HD 41004 A are summarized in Table 1, reproducing Table 1 of Santos et al. (2002). The effective temperature, surface gravity and metallicity were calculated by Santos et al. through Strömgren photometry, which also showed that the star is photometrically stable within the instrumental precision. An independent estimate of the metallicity was obtained from analysis of the Cross-Correlation Function of CORALIE. The two independent estimates of the metallicity are quoted in the table.

Table 1. Stellar parameters of HD 41004 A (reproduced from Santos et al. 2002).

Parameter	Value
Spectral Type	K1V/K2V
Parallax [mas]	23.24
Distance [pc]	43
m_v	8.65
$B-V$	0.887
$T_{\rm eff}$ [K]	5010
$\log g$ [cgs]	4.42
M_V	5.48
Luminosity [$L_\odot$]	0.65
Mass [$M_\odot$]	~0.7
$\log R'_{\rm HK}$	−4.66
Age [Gyr]	1.6
$P_{\rm rot}$ [days]	~27
$v \sin i$ [km s^{-1}]	1.22
[Fe/H]	−0.09/+0.10

The principal result of Santos et al. (2002) is the detection of a radial-velocity periodical variability in the CORALIE spectra of HD 41004. The variability pattern presented in their paper is consistent with the presence of a planet orbiting HD 41004 A with a 1.3-day period. However, Santos et al. rejected this possibility based on the bisector shape analysis of the CORALIE spectra. This analysis revealed a periodic line-shape variation, having the same period as the radial-velocity variation.

The interpretation Santos et al. suggested is the presence of an object orbiting the M2V star HD 41004 Ba. In this model A (the K star) and B are orbiting each other in a wide orbit, while B is further composed of two objects, Ba (the M star) and Bb, in a very close orbit, with a period of 1.3 days. According to this interpretation, the CORALIE spectra of HD 41004 are a combination of the A and B components, because their separation is much smaller than the diameter of the CORALIE fiber. Since the flux of the B component in the relevant wavelength range is only about 3% of the flux of the primary, large radial-velocity variations of B cause only small variations of the measured radial velocity, but their effect is manifested in the bisector shape.

Santos et al. performed some simulations to test their interpretation and concluded that their results are consistent with the presence of a brown dwarf orbiting HD 41004 Ba, with a radial-velocity amplitude of the order of 5 km s^{-1}. They also found a long-term linear trend in the radial velocities, which did not agree with the older measurements. They ascribed it to the motion of HD 41004 A around HD 41004 B, but did not rule out an additional component that may be involved in this variation.

3. Analysis

The data we analysed comprised the 86 CORALIE spectra of HD 41004 used by Santos et al. (2002), which were obtained between November 2001 and February 2002, except for one spectrum obtained in December 2000. The system was further monitored and in this paper we add 17 spectra obtained as of March 2002.

CORALIE is a fiber-fed, cross-dispersed echelle spectrograph, mounted on the 1.2-m Leonard Euler telescope at La Silla (Queloz et al. 1999). With a resolution of $\lambda/\Delta\lambda = 50\,000$, it covers the wavelength range 3800–6900 Å, with 68 echelle orders. The CORALIE system uses a software code that produces automatically the radial velocities, but for this work we used the reduced spectral orders.

The analysis used 32 CORALIE orders within the spectral range 4780–6820 Å, after having excluded the orders that are heavily polluted by telluric lines. Bluer orders were excluded because the secondary signal is expected to be too weak in these orders. Multi-order TODCOR was used to combine the correlation functions from the 32 orders. Note that the pixel-to-radial-velocity scale is different for each order. Therefore, before combining the correlation functions we had to interpolate and re-sample them into a pre-determined scale.

TODCOR requires two spectral templates as similar as possible to the expected primary and secondary spectra, and an assumed value for the flux ratio between the two spectra. We searched for the best templates in two datasets of spectra obtained by ELODIE and CORALIE. The CORALIE templates, appropriate for solar-type stars, were obtained as part of a program to derive precise abundances of planet-hosting and non-planet-hosting stars (Santos et al. 2000, 2001). The templates for the later stars were obtained using ELODIE as part of a program studying the binarity of close M dwarfs (Delfosse et al. 1998, 1999). The flux-ratio information was taken from Pickles (1998), using his measurements of typical stellar spectral energy distribution (SED), normalized according to the V-magnitude difference of HD 41004. By convolving the templates with a rotational broadening profile (e.g., Gray 1976), we created an additional degree of freedom which expanded our template library, allowing a better fit of the templates to the observed spectra.

In all the configurations of two templates that had spectral types similar to K1V and M2V, the secondary radial velocities exhibited a clear nearly circular orbit with an amplitude of around 6 km s^{-1}, and a linear trend of the primary. We finally chose the configuration which yielded the smallest residuals in the secondary velocities, relative to the best-fit orbital solution. Table 2 lists the known stellar characteristics of HD 52698 and GJ 393 – the two templates finally chosen. The stellar parameters of HD 52698 (effective temperature, surface gravity and metallicity) were derived as in Santos et al. (2001), whereas an estimate of the $v \sin i$ was obtained using the calibration of the CORALIE Cross-Correlation Function width (see the Appendix in Santos et al. 2002).

Table 2 quotes the original equatorial rotational velocities for both templates. Even mild broadening of the primary template ($v \sin i = 1$ km s^{-1}), on top of its original $v \sin i$ of 2 km s^{-1}, degraded the solution considerably. On the other hand, the secondary template could be broadened by $v \sin i$ up to 5 km s^{-1} without significantly affecting the solution. Finally we used a broadening of $v \sin i = 1$ km s^{-1}, which yielded the smallest residuals of the secondary velocities.

Table 2. Known stellar characteristics of the templates finally chosen.

Parameter	Primary Template	Secondary Template
Name	HD 52698	GJ 393
Spectral Type	K1[1]	M2.5[1]
$B-V$	0.89[1]	1.52[1]
$T_{\rm eff}$ [K]	5235	N/A
$\log g$	4.69	N/A
[Fe/H]	0.21	N/A
$v \sin i$ [km s^{-1}]	2.0	< 2.9[2]

1. Hünsch et al. 1999.
2. Delfosse et al. 1998.

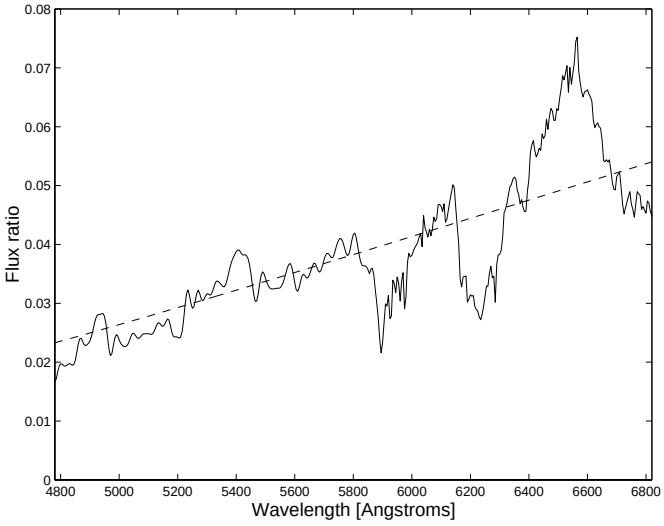

Fig. 1. The flux ratio in the relevant wavelength range, calculated according to Pickles (1998). The dashed line represents the flux ratio corresponding to black-body radiation laws of 3500 K and 5240 K.

Figure 1 shows the flux ratio as a function of wavelength, corresponding to the chosen spectral types of K1V and M2.5V, using the SED library of Pickles (1998). The dashed line in the figure shows the flux ratio obtained by assuming a black-body radiation law for the two spectra, with a temperature of 3500 K for the secondary. It is clear that while the black-body model roughly fits the detailed flux-ratio, it is not accurate enough and there are large differences, e.g., around 6500 Å. In any case, using a constant flux ratio as in the single-order application of TODCOR is clearly not sufficient for such a wide spectral range.

Figure 2 demonstrates the way multi-order TODCOR measures the radial velocity of HD 41004 B. The figure presents one-dimensional "cuts" of the two-dimensional correlation function. In each "cut" the correlation is shown as a function of the secondary velocity, while the primary velocity is fixed according to the location of the two-dimensional maximum.

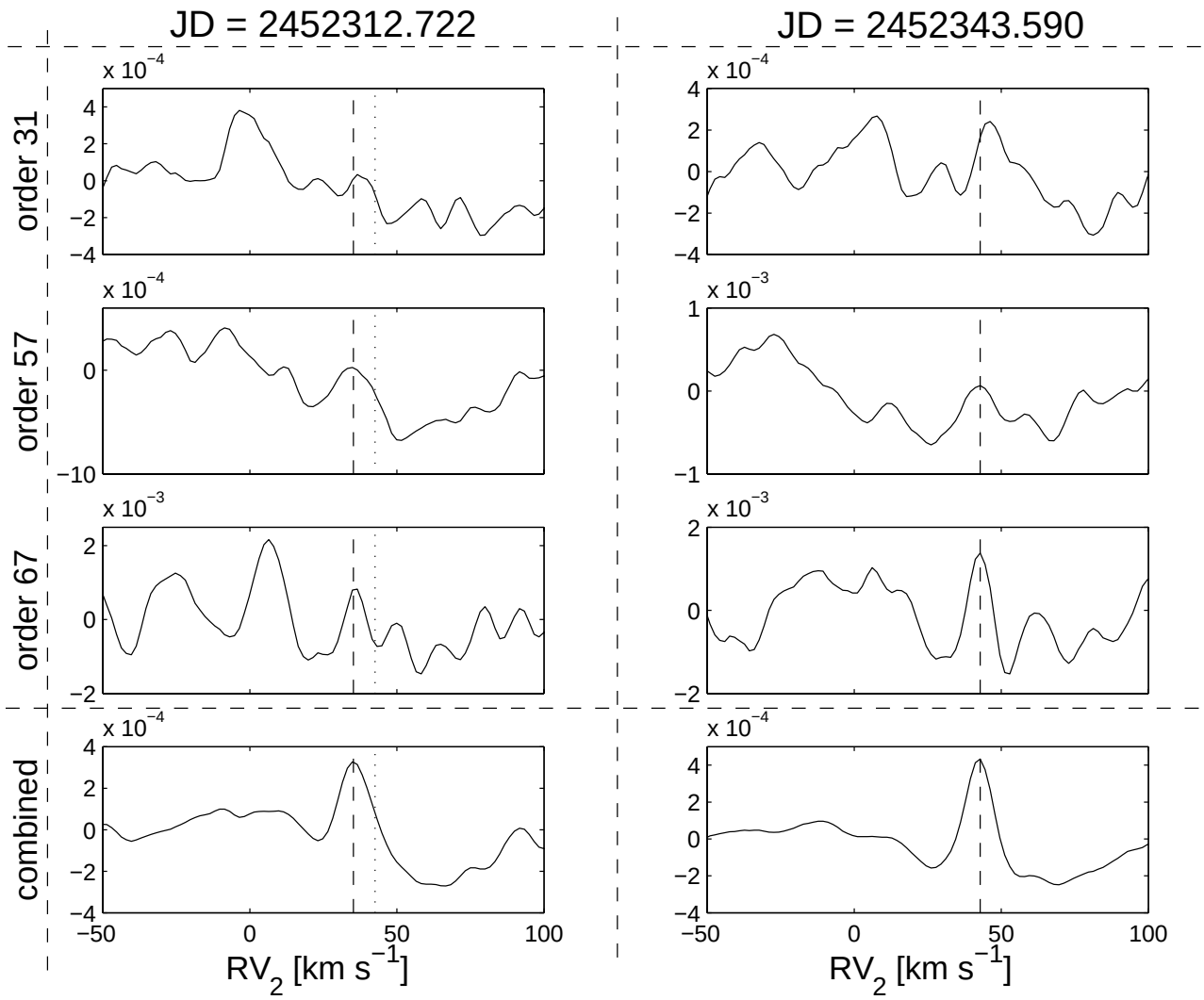

Fig. 2. The upper three panels in each column show "cuts" (see text) of the two-dimensional correlation function for three selected orders. The dashed lines represent the best-fit secondary velocities while the dotted lines represent the primary velocity. It is not shown on the right column where it almost coincides with the secondary velocity. The lower panel in each column shows the "cut" of the function obtained after combining the corresponding correlation functions of all the 32 orders. A third-order best-fit polynomial was subtracted from all the shown functions to accentuate the local peak.

Because of the small flux-ratio between the two templates, we expect the correlation value to change very little when the secondary template alone is shifted. However, in each "cut" we still expect to see a relative peak around the correct secondary velocity. The figure is divided into two columns, corresponding to two different exposures (JD = 2 452 312.722 and JD = 2 452 343.590). Using the best-fit orbit, the expected secondary velocity for the spectrum used in the left column of the figure is 35.2 km s^{-1}, while for the right column it is 42.2 km s^{-1}. These velocities are marked on the figure by dashed lines. The primary velocity is represented by a dotted line in the left column, while in the right column it almost coincides with the secondary velocity. For this graphic demonstration only, a third-order best-fit polynomial was subtracted from all the plotted functions in order to accentuate the local peak.

The three upper panels in each column demonstrate the problems in the single-order TODCOR. On the left, the first upper panel exhibits a very prominent peak in a wrong velocity. The second and third panels show a moderate peak at about the expected velocity In almost all 32 orders, some local peaks appeared around the correct velocity. The lower panel shows the result of combining the correlation functions of all the analysed orders. The correct peak is clearly emphasized relative to the spurious peaks.

Comparing the two columns of Fig. 2, we see that we cannot know in advance which orders present the correct peak. Thus, we have to combine all 32 orders in order to have the correct peak emphasized. The right column of the Figure demonstrates another advantage of TODCOR: in this spectrum the secondary velocity is almost identical to the primary velocity. In the conventional one-dimensional cross-correlation, there is no way to measure the two velocities, due to the blending of the two correlation peaks. TODCOR, by using two different templates, allows the measurement of both velocities.

Table 3. Best-fit orbital solution of HD 41004 B.

P	[days]	1.328199	± 0.000081
T	[JD]	2 452 339.212	± 0.040
e		0.065	± 0.014
γ	[km s^{-1}]	41.631	± 0.057
ω	[°]	171	± 11
K	[km s^{-1}]	6.192	± 0.081
$a \sin i$	[10^{-3} AU]	0.7544	± 0.0098
$f(m)$	[$10^{-6}\,M_\odot$]	32.5	± 1.3
$M^{\dagger}_{\rm Bb,min}$	[$M_{\rm J}$]	18.64	± 0.26
N		103	
$\sigma_{\rm O-C}$	[km s^{-1}]	0.56	

†Assuming $M_{\rm Ba} = 0.4\,M_\odot$.

The listing of the radial velocities of A and B and the corresponding times, can be obtained at the CDS.

4. Results

Figure 3 shows the resulting orbit of HD 41004 B, while the orbital elements are summarized in Table 3. Applying multi-order TODCOR to many orders (32), combined with the large number of measurements (103) yielded a very precise orbital solution. Thus, the radial-velocity amplitude (K) was found with a precision of about 1%. This fine precision allowed also a very accurate estimate of the orbital eccentricity (e). Although very small, the eccentricity is still non-vanishing, with a significance level of 2×10^{-5} according to the Lucy & Sweeney (1971) test. Assuming a mass of ∼0.4 $M_\odot$ for HD 41004 Ba, the companion minimum mass is 19 $M_{\rm J}$. The uncertainty of 0.26 $M_{\rm J}$ does not take into account the uncertainty in the mass of HD 41004 Ba – $M_{\rm Ba}$. A 20% uncertainty in $M_{\rm Ba}$ would result in a 2.3 $M_{\rm J}$ uncertainty in $M_{\rm Bb,min}$.

Figure 4 shows the velocities of HD 41004 A. The velocities measured after JD = 2 452 200 show a clear linear trend. The best-fit line has a slope of +105 ± 10 m s^{-1} year^{-1}, and is also shown in the Figure. As Santos et al. (2002) have already noticed, the first isolated measurement does not agree with the linear trend implied by the other measurements. A Lomb-Scargle periodogram of the de-trended velocities (Fig. 5) shows no hint of the 1.3-day periodicity, again proving that only the B component participates in the periodic motion, as suggested by Santos et al. (2002). In light of the trend in the velocities of component A, we tried also to fit the B velocities with an additional trend but the resulting trend was not statistically significant.

The mean radial velocity of A during the linear part is 42.5768 ± 0.0009 km s^{-1}, which is very close to the center-of-mass velocity of B – the difference is only $\Delta RV = 0.95 \pm 0.06$ km s^{-1}. However, this difference depends also on the estimated velocities we used for the templates, and therefore we adopt a conservative error estimate of 0.1 km s^{-1} for ΔRV.

5. Discussion

The radial velocities derived in the previous section support the triple-system model suggested by Santos et al. for HD 41004.

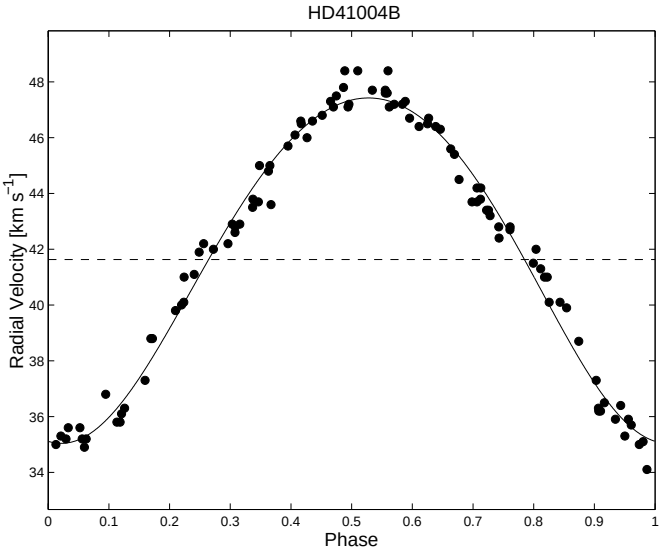

Fig. 3. Phased radial velocities of HD 41004 B.

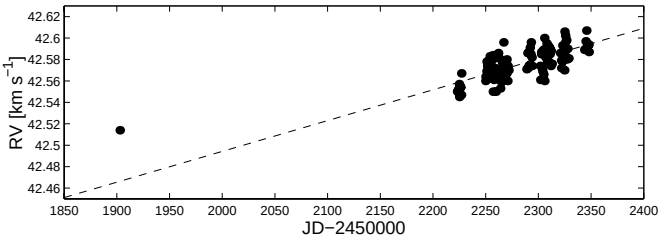

Fig. 4. Radial velocities of HD 41004 A. The dashed line is the best fit to the velocities, ignoring the first isolated velocity.

Our results allow, nevertheless, a somewhat more detailed study of the system.

5.1. The long-term trend of the radial velocity of HD 41004 A

As we have demonstrated in the previous section (see Fig. 4), the radial velocities of HD 41004 A show a clear long-term variation over time. For the period November 2001 to February 2002 this variation can be nicely fitted by a linear increase. Note, however, that one single point, at JD = 2 451 902.774, which was observed one year before all the others – on December 2000, deviates substantially from this linear fit. This point may indicate that the extrapolation of the linear approximation is no longer valid for the time of that point. Thus, we may actually be seeing the curved part of a long-term orbit, caused by a fourth component in the system. Such an object would have an orbital motion with a much shorter period than that of the AB system, which is at least 100 years, as inferred from the observed separation. In fact, follow-up measurements we are currently performing hint that this may indeed be the case, but a detailed solution of the orbit would still be premature.

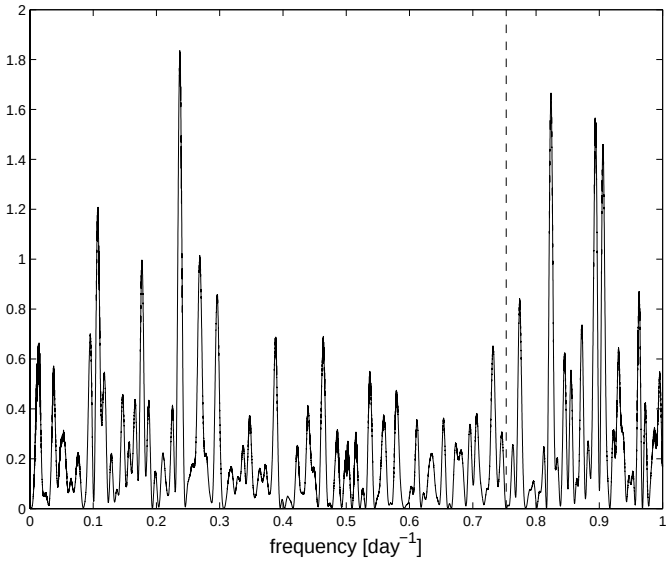

Fig. 5. Lomb-Scargle periodogram of the velocities of HD 41004 A after subtracting the linear trend. The dashed line marks the frequency corresponding to the 1.3-day period of HD 41004 B.

5.2. The close orbit and the rotation of HD 41004 Ba

As mentioned in Sect. 3, the process by which we chose the templates allows a very crude estimate of the equatorial rotational velocity. The best-fit orbit was attained when the M2 template was convolved with a rotation profile of $v \sin i = 1\,\mathrm{km\,s^{-1}}$. Our procedure is not accurate enough to use this value as a true measurement of $v \sin i$. However, trying large values for $v \sin i$ degraded the quality of the orbital solution. For example, while the quality of the solution remained almost unchanged for $v \sin i$ as large as $5\,\mathrm{km\,s^{-1}}$, the O–C RMS was doubled at $v \sin i = 10\,\mathrm{km\,s^{-1}}$. Thus, we believe that the equatorial velocity of Ba is of the order of a few $\mathrm{km\,s^{-1}}$, and probably less than $10\ \mathrm{km\,s^{-1}}$. Even this crude estimate is sufficient to conclude that $v \sin i$ is substantially lower than the expected equatorial velocity of $\sim 20\,\mathrm{km\,s^{-1}}$, assuming synchronization (Santos et al. 2002).

At such a close orbit, with a period of 1.33 days, it is usually assumed that synchronization and alignment of the spin with the orbital motion had been established (Santos et al. 2002). An obvious explanation of the apparently small $v \sin i$ would be small orbital inclination. Assuming alignment, small inclination implies that the mass of the unseen companion is considerably larger than its derived minimum value.

5.3. The small eccentricity of the close orbit

A binary or a star-planet system with a period as short as 1.33 days is naïvely believed to have been circularized. However, our radial-velocity solution shows that the close orbit has a finite non-zero eccentricity – $e = 0.065 \pm 0.014$, which has to be explained.

Let us first estimate the timescale of circularization due to processes occurring in Ba. The relevant process is dissipation of the equilibrium tide through interaction with the convective envelope (Zahn 1989). We follow Rasio et al. (1996) and write:

$$\tau_{\mathrm{circ}} = \frac{\tau_{\mathrm{c}}}{f} \frac{M}{M_{\mathrm{env}}} \frac{1}{q(1+q)} \left(\frac{a}{R}\right)^8,$$

where the parameter $\tau_{\mathrm{c}} \approx (MR^2/L)^{\frac{1}{3}}$ is the eddy turnover timescale, and its numerical value is about 0.5 yr. The numerical value of f is obtained by integrating the viscous dissipation of the tidal energy through the convective zone and is of order unity (Zahn 1977). In our case the tidal pumping period – $P/2$ – is much smaller than τ_{c}, and therefore only convective eddies with turn-over time less than $P/2$ contribute to the dissipation. The value of f is then reduced to $(P/(2\tau_{\mathrm{c}}))^{\alpha}$ (Zahn 1989). The correct value of α is debated but generally assumed to be either 1 (Zahn 1992) or 2 (Goldreich & Keeley 1977; Goldman & Mazeh 1991). We assume that the mass of the convective envelope – M_{env} – is very close to the stellar mass – M (e.g., Chabrier & Baraffe 2000). The resulting timescale is about 10^{10} yr, assuming $\alpha = 1$, and certainly much larger if $\alpha = 2$. At the age of 1.5 Gyr, it therefore seems that circularization through dissipation in Ba has not taken place.

Now let us examine the possible involvement of Bb in circularization processes. If the object is substellar or maybe even a very late M-dwarf, radiative zones in the atmosphere may form either due to the internal physics (Burrows et al. 1997) or due to the external heating by the primary (Guillot et al. 1996). These would necessitate another approach to calculate the circularization timescale, probably based on dissipation of the dynamical tide (Zahn 1977). The theory of orbital evolution through tidal dissipation is still debated, specially the mechanisms for dissipation of the dynamical tide (e.g., Claret et al. 1995), and therefore it is not clear whether it contributes significantly in the case of HD 41004 B.

6. Conclusion

We have presented in this work the first application of multi-order TODCOR to echelle spectra. The case of HD 41004 demonstrates the unique capabilities of this technique. It utilizes all the available prior knowledge regarding *both* spectral components (the different templates), it is not limited to a fixed flux ratio (we used the SED to calculate it) and it incorporates optimally the data from all the relevant spectral orders. Based on the best-fit solutions of the present case, we estimate the precision of the secondary velocity of HD 41004 to be $0.56\,\mathrm{km\,s^{-1}}$ and that of the primary velocities to be $10\,\mathrm{m\,s^{-1}}$. The radial velocities yielded accurate orbital elements of the unseen companion of HD 41004 B, and an accurate measurement of the radial acceleration of HD 41004 A. The latter suggested an additional component may be present in the system. Follow-up observations, currently underway, tend to confirm this hypothesis.

The combination of multi-order TODCOR together with the high signal-to-noise and high resolution of the CORALIE spectra render this analysis a very promising path toward expanding the database of spectroscopic binaries and multiple systems (like HD 41004). It may also facilitate the detection

of planets in binary stellar systems, which are lately the focus of an increasing interest.

Acknowledgements. This research was supported by the Israeli Science Foundation (grant no. 40/00). Support from Fundação para a Ciência e Tecnologia, Portugal, to N.C.S. in the form of a scholarship is gratefully acknowledged.

References

Burrows, A., Marley, M., Hubbard, W. B., et al. 1997, ApJ, 491, 856
Chabrier, G., & Baraffe, I. 2000, ARA&A, 38, 337
Claret, A., Gimenez, A., & Cunha, N. C. S. 1995, A&A, 299, 724
Delfosse, X., Forveille, T., Beuzit, J.-L., et al. 1999, A&A, 344, 897
Delfosse, X., Forveille, T., Perrier, C., & Mayor, M. 1998, A&A, 331, 581
Goldman, I., & Mazeh, T. 1991, ApJ, 376, 260
Goldreich, P., & Keeley, D. A. 1977, ApJ, 211, 934
Gray, D. F. 1976, The observation and analysis of stellar photospheres (New York: Wiley-Interscience)
Guillot, T., Burrows, A., Hubbard, W. B., Lunine, J. I., & Saumon, D. 1996, ApJ, 459, L35
Hünsch, M., Schmitt, J. H. M. M., Sterzik, M. F., & Voges, W. 1999, A&AS, 135, 319
Lucy, L. B., & Sweeney, M. A. 1971, AJ, 76, 544
Mazeh, T., Prato, L., Simon, M., et al. 2002, ApJ, 564, 1007
Mazeh, T., & Zucker, S. 1994, Ap&SS, 212, 349
Pickles, A. J. 1998, PASP, 110, 863
Prato, L., Simon, M., Mazeh, T., et al. 2002, ApJ, 569, 863
Queloz, D., Casse, M., & Mayor, M. 1999, in IAU Colloq. 170: Precise Stellar Radial Velocities, ASP Conf. Ser., 185, 13
Rasio, F. A., Tout, C. A., Lubow, S. H., & Livio, M. 1996, ApJ, 470, 1187
Santos, N. C., Israelian, G., & Mayor, M. 2000, A&A, 363, 228
Santos, N. C., Israelian, G., & Mayor, M. 2001, A&A, 373, 1019
Santos, N. C., Mayor, M., Naef, D., et al. 2002, A&A, 392, 215
Simkin, S. M. 1974, A&A, 31, 129
Tonry, J., & Davis, M. 1979, AJ, 84, 1511
Zahn, J.-P. 1977, A&A, 57, 383
Zahn, J.-P. 1989, A&A, 220, 112
Zahn, J.-P. 1992, in Binaries as Tracers of Stellar Formation., ed. A. Duquennoy, & M. Mayor (Cambridge: Cambridge University Press), 253
Zucker, S. 2003, MNRAS, in press [astro-ph/0303426]
Zucker, S., & Mazeh, T. 1994, ApJ, 420, 806